Available online at www.sciencedirect.com
ScienceDirect
European Journal of Medicinal Chemistry 44 (2009) 179–189
EUROPEAN JOURNAL OF MEDICINAL CHEMISTRY
http://www.elsevier.com/locate/ejmech

Original article

Synthesis and activity of fibrillogenesis peptide inhibitors related to the 17–21 β-amyloid sequence

Cesare Giordano [a,*], Annalisa Masi [b], Aldo Pizzini [b], Anna Sansone [b], Valerio Consalvi [c], Roberta Chiaraluce [c], Gino Lucente [b]

[a] *Istituto di Chimica Biomolecolare del CNR, Università ''La Sapienza'', P.le A. Moro 5, 00185 Roma, Italy*
[b] *Dipartimento di Studi Farmaceutici, Università ''La Sapienza'', P.le A. Moro 5, 00185 Roma, Italy*
[c] *Dipartimento di Scienze Biochimiche, Università ''La Sapienza'', P.le A. Moro 5, 00185 Roma, Italy*

Received 31 October 2007; received in revised form 21 February 2008; accepted 20 March 2008
Available online 8 April 2008

Abstract

Peptide derivatives **1**–**5**, incorporating synthetic non-proteinogenic amino acids, related to the β-amyloid 17–21 fragment of the amyloidogenic $A\beta_{1-40}$, and the *N*-protected decapeptide **6**, corresponding to a dimeric sequence of the same fragment, have been synthesized. These compounds were designed by using Soto's pentapeptide Ac–LPFFD–NH_2 (iAβ5p) as lead compound. Their activity as inhibitors of fibrillogenesis and stability against enzymatic degradation have been determined. Compounds **1**, **5** and **6** are potent inhibitors in comparison to the lead compound. Exposure to chymotrypsin of peptide derivatives **1**–**5**, all containing unnatural amino acids, shows increased stability as compared with iAβ5p and **6**. Conformational properties of the new compounds have been determined by CD and FT-IR spectroscopies.

Keywords: Alzheimer's disease; β-Amyloid; Fibrillogenesis; Aggregation inhibitor; Fluorescence assay; Scanning electron microscopy

1. Introduction

Amyloidoses are a class of diseases in which soluble proteins or peptides accumulate in the form of amyloid aggregates which are deposited as plaques in the extracellular space. Plaques are commonly observed in diseases of completely unrelated origin, such as Parkinson's disease, type II diabetes, prion disorders and Alzheimer's disease (AD). AD is the most common form of dementia in adults and the neuritic plaques in the brain contain extracellular deposit of amyloid β-protein (Aβ) [1,2]. Aβ is composed of a 39–43 amino acid long peptide produced by cleavage from a larger amyloid precursor protein (APP). The amyloid fibril formation and deposit are due to conformational switching from α-helical to β-sheet structure during amyloidogenesis [1]. On this basis, a rational pharmacological approach for prevention of amyloid formation and deposit would be to find compounds able to specifically stabilize the α-helical conformations [3] and/or destabilize the β-sheet conformations of the amyloidogenic protein [4,5]. Several recent papers deal with this topic trying to gain insight into the mechanism of amyloid fibril formation and the role played by different factors such as H-bonding, peptide backbone chirality and composition [6–12].

The design of a therapeutic strategy against this pathology initiated from the observation that short synthetic peptides are capable to interact with Aβ without becoming part of β-sheet structure. These synthetic peptides, named β-sheet breaker peptides (BSBp), may destabilize the amyloidogenic Aβ conformer and hence preclude amyloid formation [13].

Since fibril formation could be impaired by substitution of hydrophilic for hydrophobic residues in the hydrophobic region of the $A\beta_{1-40}$ sequence [14], we chose as model of

Abbreviations: DMF, dimethylformamide; EDC, *N*-(3-dimethylaminopropyl)-*N*′-ethylcarbodiimide hydrochloride; EDT, ethane dithiol; HOBT, 1-hydroxybenzotriazole; PBS, phosphate buffer saline; SEM, scanning electron microscopy; TEA, triethylamine; TFA, trifluoroacetic acid; TPS, triisopropylsilane.

* Corresponding author. Tel.: +39 06 49913237; fax: +39 06 491491.
E-mail address: cesare.giordano@uniroma1.it (C. Giordano).

0223-5234/$ - see front matter © 2008 Elsevier Masson SAS. All rights reserved.
doi:10.1016/j.ejmech.2008.03.036

inhibitor the synthetic five-residue β-sheet-breaker peptide derivative Ac–Leu-Pro-Phe-Phe-Asp(OH)–NH_2 (Ac–LPFFD–NH_2; iAβ5p). This compound, previously reported by Soto and coworkers [15], in addition to *N*- and *C*-terminal protections has a proline and an aspartic residue which substitute valine and alanine, respectively, in the 17–21 (LVFFA) fragment of the 1–40 sequence and possesses a series of promising properties: it has been shown to cross the blood–brain barrier, to inhibit (and disassemble) the formation of amyloid fibrils in vitro and in vivo, to prevent Aβ neurotoxicity in cell culture, to arrest amyloid deposition and to induce dissolution of preformed plaques in rat brain model of amyloidosis [5,16,17]. Particularly effective in determining the iAβ5p behaviour is the incorporation of the proline residue, a strategy commonly used to induce secondary structures and inhibit β-sheet formation. It is worth noting in this context that incorporation of proline in two series of Aβ fragments ($Aβ_{15–23}$ and $Aβ_{12–26}$) showed that residues 17–23 make up the β-sheet core of these fragments [18].

The iAβ5p molecule has been adopted by Soto's group as lead compound and several strategic chemical modifications have been applied in order to improve its activity and metabolic stability [15]. C^{α}-Carbon and *N*-amide bond methylation showed that the major cleavage site by peptidases is at the Pro–Phe bond. Furthermore, substitution of these two amino acids with unnatural residues was found to be highly detrimental for in vitro activity in all examined derivatives. Replacement of Pro with cysteine-derived pseudoproline residues, able to stabilize *cis* conformation around the CO–N bond, decreased the activity, thus suggesting that *trans* configurated CO–Pro amide bond is required for the activity. Furthermore, replacement of the *N*-terminal acetyl group with residues of *N*-methylglycine (sarcosine, Sar) or *N*,*N*-dimethylglycine (*N*-methylsarcosine, MeSar), leading to Sar–LPFFD–NH_2 and MeSar–LPFFD–NH_2, resulted in a decrease of peptidase recognition and high activity against fibrillogenesis [15].

The design of the pseudopeptides in this report aimed to disrupt the hydrogen bonding that stabilizes the β-structure of fibrillar amyloid aggregates. Furthermore, taking into account the short half-life of peptides in circulation, we focused also on the possibility to obtain more stable sequences taking into account the position-2 sensitivity of iAβ5p toward proteolysis. According to the above considerations, we synthesized the analogues **1**–**6** of the iAβ5p reported in Table 1.

Compounds **1**–**4** maintain the original sequence and protecting groups of iAβ5p with the exception of substitutions at Pro residue. The four-membered azetidine skeleton was incorporated in analogues **1** and **2**; in particular (see Scheme 1) compound **1** contains the residue of (*S*)-azetidine-2-carboxylic acid (Aze) while in **2** the (2*R*,3*R*)-*trans*-3-phenyl substituted analogue (PhAze) was incorporated. As compared to Pro, peptides containing the smaller ring of Aze show comparable behaviour toward the *cis*–*trans* isomerism but higher backbone flexibility due to the lower steric interference exerted by the ring atoms [19]. The more constrained ring of the Aze should, however, maintain and probably accentuate some of the expected consequences of the Pro residue incorporation, such as alteration of the backbone conformation and incompatibility with the peptide bond geometries found in the β-sheet bonding network. In analogues **3** and **4** the Pro residue was homologated to give a β-amino acid structure. Compound **3** contains (*S*)$β^3$-HPro [20] while in analogue **4** the Pro homologation has been combined with the replacement of the carboxyl with a sulfonyl group, thus generating a sulfonamide junction and an α-peptide/β-peptidosulfonamide hybrid [21,22]. As it is well documented, the incorporation of β-aminocarboxylic or β-aminosulfonic acid residues into natural peptides has profound effect on both backbone conformation and metabolic stability. In particular, sulfonamido-β-peptides and related α/β hybrids represent a very attractive class of compounds due to the peculiar chemical and structural properties of the SO_2–N(R) junction. This bond, which is completely stable to proteases and possesses two negatively charged oxygen atoms directly bound to the tetrahedral sulfur, can significantly alter polarity and H-bonding patterns of the native counterparts. The approach based on the incorporation of a CH_2–SO_2–NH junction, replacing the usual CO–NH peptide bond, has also been applied in the case of compound **5**. This latter compound resembles the iAβ5p analogue (MeSar–LPFFD–NH_2) previously studied by Soto's group [15] and contains, as *N*-terminal residue, *N*,*N*-dimethyl-taurine (*N*,*N*-dimethy-2-aminoethanesulfonic acid; Me_2Tau) residue in place of *N*,*N*-dimethylglycine (Me_2Gly or MeSar). Finally, in a different approach compound **6** has been synthesized. This is the iAβ5p dimer in which the Ac–LPFFD–OH unit has been joined to the *N*-terminal group of the pentapeptide LPFFD–NH_2 giving rise to the *N*-protected decapeptide derivative **6**.

Table 1
Sequence and mass spectra analysis of iAβ5p and its synthetic analogues

Peptide	Sequence[a]	M (Na^+) obsd (MW calcd)
iAβ5p	Ac–Leu-Pro-Phe-Phe-Asp(OH)–NH_2[b]	701.5302 (678.3533)
1	Ac–Leu-**Aze**-Phe-Phe-Asp(OH)–NH_2	687.1848 (664.3220)
2	Ac–Leu-(2*R*,3*R*)-**PhAze**-Phe-Phe-Asp(OH)–NH_2	763.3305 (740.3533)
3	Ac–Leu-**β-HPro**-Phe-Phe-Asp(OH)–NH_2	715.2387 (692.3533)
4	Ac–Leu-**Pro-ψ[CH_2SO_2]**-Phe-Phe-Asp(OH)–NH_2	751.1428 (728.3203)
5	**Me_2Tau**-Leu-Pro-Phe-Phe-Asp(OH)–NH_2	794.0246 (771.3625)
6	Ac–Leu-Pro-Phe-Phe-Asp(OH)-Leu-Pro-Phe-Phe-Asp(OH)–NH_2	1321.5274 (1297.6383)

[a] Modifications are shown in bold letters.
[b] See Ref. [15].

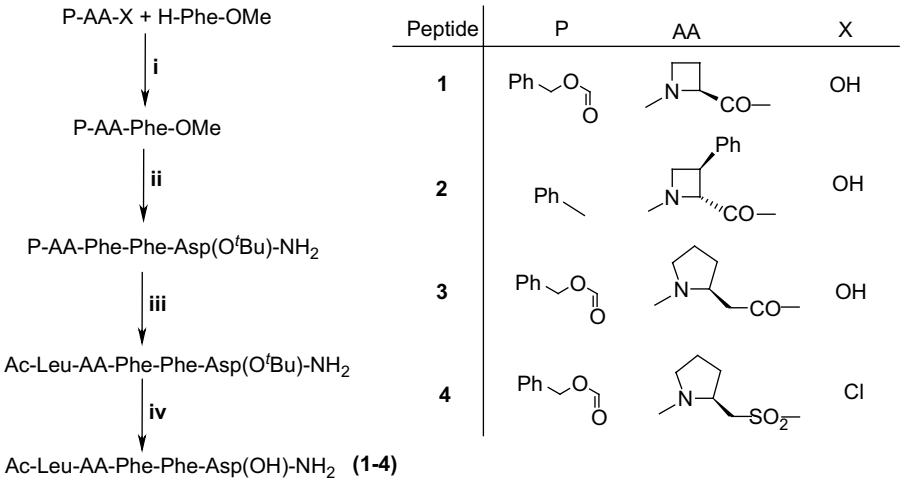

Scheme 1. Synthesis of pseudopeptides **1**–**4**. Reagents: (i) for **1**–**3**: EDC, HOBt, TEA, DCM; for **4**: TEA, DCM; (ii) a: 2 N NaOH, MeOH; b: H–Phe-Asp(O^{t}Bu)–NH_2, EDC, HOBt, TEA, DCM; (iii) a: for **1**, **3** and **4**: H_2/Pd–C, TFA, MeOH; for **2**: 4% formic acid in MeOH, Pd black; b: Ac–Leu–OH, EDC, HOBt, TEA, DCM; (iv) TFA.

2. Results

2.1. Chemistry

Preparation of peptides **1**–**5** was performed by conventional methods in solution, using the carbodiimide method for coupling steps, except for the sulfonamido derivatives which were obtained by using sulfonylchlorides. For the synthesis of the pseudopeptides **1**–**4** (Scheme 1), the *N*-protected pseudoaminoacid (P–AA–X) was coupled with Phe–OMe and the resulting dipeptide methylester was subjected to alkaline hydrolysis. Successive coupling with Phe-Asp(O^{t}Bu)–NH_2 gave the tetrapeptide which was *N*-deprotected and coupled with Ac–Leu–OH.

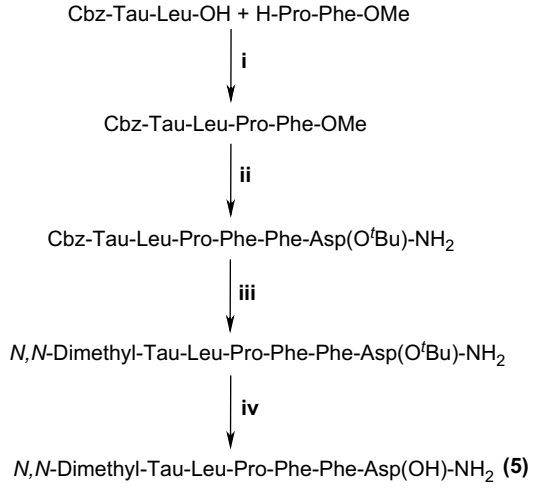

Scheme 2. Synthesis of pseudopeptide **5**. Reagents: (i) EDC, HOBt, TEA, DCM; (ii) a: 2 N NaOH, MeOH; b: H–Phe-Asp(O^{t}Bu)–NH_2, EDC, HOBt, TEA, DCM; (iii) a: H_2/Pd–C, TFA, MeOH; b: $(CH_2O)_n$/$NaBH_4CN$, MeCN; (iv) TFA.

For the synthesis of peptide **5** (Scheme 2), Cbz–Tau-Leu–OH was coupled with Pro-Phe–OMe. The tetrapeptide was then subjected to alkaline hydrolysis and coupled with Phe-Asp(O^{t}Bu)–NH_2. After *N*-deprotection by catalytic hydrogenation, the taurine-containing peptide was *N*,*N*-dimethylated by reductive alkylation with 35% aqueous formaldehyde and sodium cyanoborohydride [23].

Treatment with TFA afforded the required final free peptides. All peptides were purified by HPLC and characterized by mass spectrometry (see Table 1). (2*R*,3*R*)-(1-Benzyl-3-phenyl-azetidine-2-yl)-carboxylic acid hydrochloride, required for the synthesis of the peptide **2**, was prepared starting from (*R*)-phenylglycinol according to a published procedure [24]. The Cbz–(*S*)-β-homoproline-derived sulfonylchloride (Cbz–Pro–ψ[CH_2SO_2]–Cl) **3**, required for the preparation of the peptide **4**, was synthesized according to Scheme 3 starting from the corresponding sulfonic acid **1** [25]. After *N*-protection with benzyl-chloroformate, the sodium salt **2** was converted into the corresponding sulfonylchloride **3** by treatment with phosgene [26].

The peptide iAβ5p and its analogue **6** were synthesized by Fmoc solid-phase synthetic protocols on Rink-amide resin according to standard protocols [27]. The crude peptides were purified by RP-HPLC using a Bondapac C-18 column (1.9 × 30 cm) with elution at 8 mL/min by a linear gradient of 10–60% acetonitrile in 0.1% aqueous trifluoroacetic acid in 30 min.

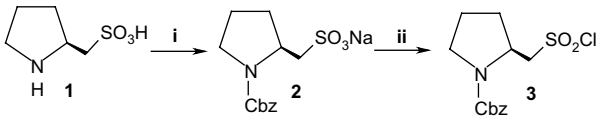

Scheme 3. Synthesis of derivative **3**. Reagents: (i) Cbz–Cl, 1 N NaOH; (ii) $COCl_2$/toluene.

2.2. In vitro activity and stability

The in vitro inhibitory activity of the new analogues **1**–**6** toward amyloid fibril formation has been determined by an amyloid-specific dye binding analysis and compared with that of a sample of the reference model iAβ5p under the same conditions (Fig. 1). The quantitative evaluation of the effect of compounds **1**–**6** on in vitro fibrillogenesis was performed with thioflavin T (ThT), a fluorescent dye, which associates with amyloid fibrils with a concomitant fluorescence enhancement in response to the fibril aggregation grade [28]. The preparation of $A\beta_{1-40}$ according to Fezoui et al. [29] allowed us to easily obtain fibril formation reactive to ThT on a 24-h time scale. The first experimental data point was taken after 30 min incubation of $A\beta_{1-40}$ in the absence or presence of inhibitors (Fig. 1A). In order to decrease the experimental error due to sample evaporation, the incubation was carried out at 20 °C for a maximum time of 24 h. The results are shown in Fig. 1A and compared with the fibril formation in the absence of inhibitor and in the presence of iAβ5p under the same conditions. A bar plot (Fig. 1B) of the amount of fibril formation after 24 h incubation of the $A\beta_{1-40}$ fraction in the presence of the inhibitors indicates that compounds **1**, **5** and **6** show activity 1.2-, 1.5- and 2.2-fold higher than iAβ5p, respectively, while compounds **2**–**4** do not show any significant inhibition of $A\beta_{1-40}$ fibril formation (data not shown).

The effect of inhibitors on $A\beta_{1-40}$ fibrillogenesis was studied also by electron microscopy. Fig. 2 shows SEM images of $A\beta_{1-40}$ after incubation at 20 °C in the absence (Fig. 2A and B) and presence (Fig. 2C and D) of compound **5**. In the absence of the inhibitor, $A\beta_{1-40}$ sample shows the formation of protofibrils less than 1 μm in length [30,31] which become more clearly visible after 24 h incubation (Fig. 2B). In the presence of the inhibitor (Fig. 2C and D), the protofibrils as well as any kind of fibrillar structure are absent; the few globular structures visible do not show any morphological resemblance of amyloid aggregates and are presumably formed by the inhibitor, as suggested by SEM images of the inhibitor alone (data not shown).

In agreement with the experimental hypothesis, the modification of the residues more exposed to the proteolytic cleavage increases the resistance of the compound to proteolysis (Fig. 3). The iAβ5p analogues **1**–**5**, all containing unnatural amino acids, after exposure to chymotrypsin show, under the adopted experimental conditions, increased stability in comparison with the parent peptide iAβ5p and to its decapeptide analogue **6**. After 2 h incubation at 37 °C, only 12 and 22% of iAβ5p and peptide **6**, respectively, were detected, while 35–45% of the pseudopeptides **1**–**4** and 70% of the pseudopeptide **5** survived. After 20 h incubation, the iAβ5p and the peptide **6** were near totally degraded, while 15–20% of analogues **1**–**4** and 55% of analogue **5** remained intact. The analogue **6** together with the unmodified iAβ5p model, both containing only proteinogenic residues, shows the expected lowest stability toward enzymatic degradation.

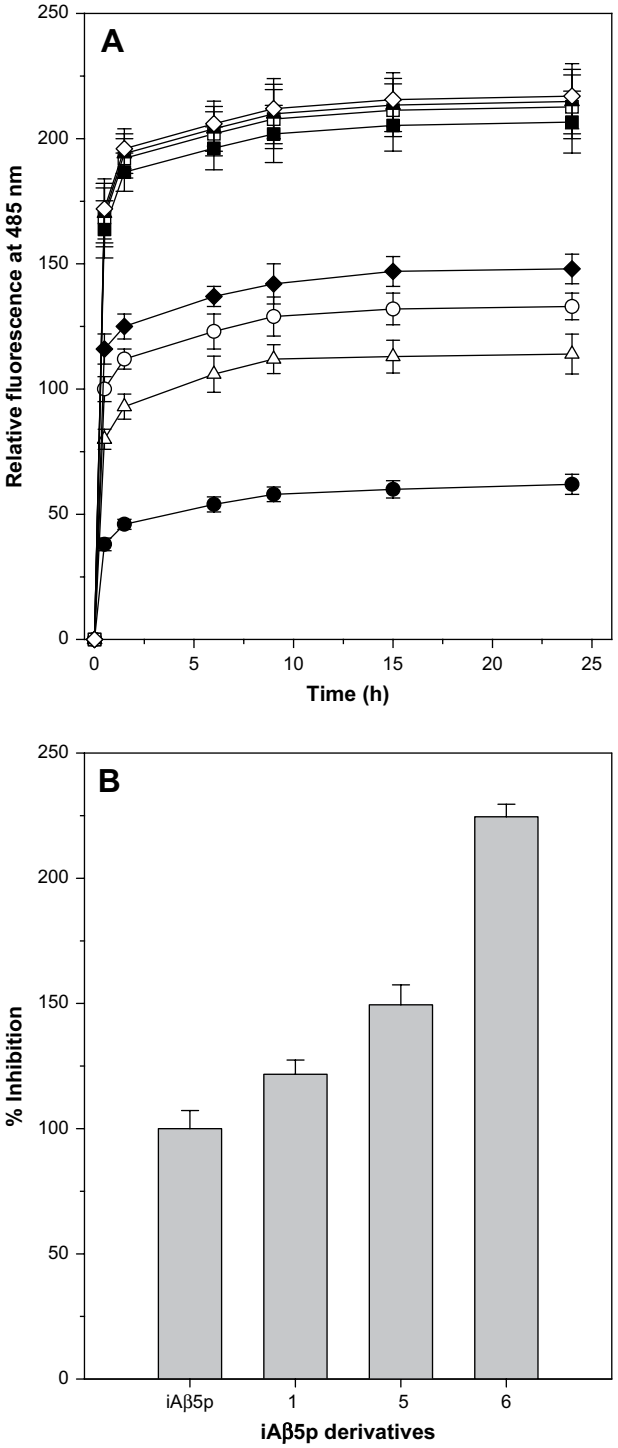

Fig. 1. In vitro activity of iAβ5p derivatives **1**–**6**. All compounds were tested for activity using the ThT fluorescent assay for quantification of amyloid fibril formation by $A\beta_{1-40}$. (A) $A\beta_{1-40}$ fraction (about 100 μg) was incubated in 100 μL of 30 mM Tris/HCl buffer at pH 7.4 at 20 °C with and without 10 M excess of the synthesized compound (◇ control, ○ **1**, ■ **2**, □ **3**, ▲ **4**, △ **5**, • **6**, ◆ iAβ5p). (B) Values correspond to the percentage of inhibition of amyloid formation and are expressed relative to the activity of iAβ5p (100%).

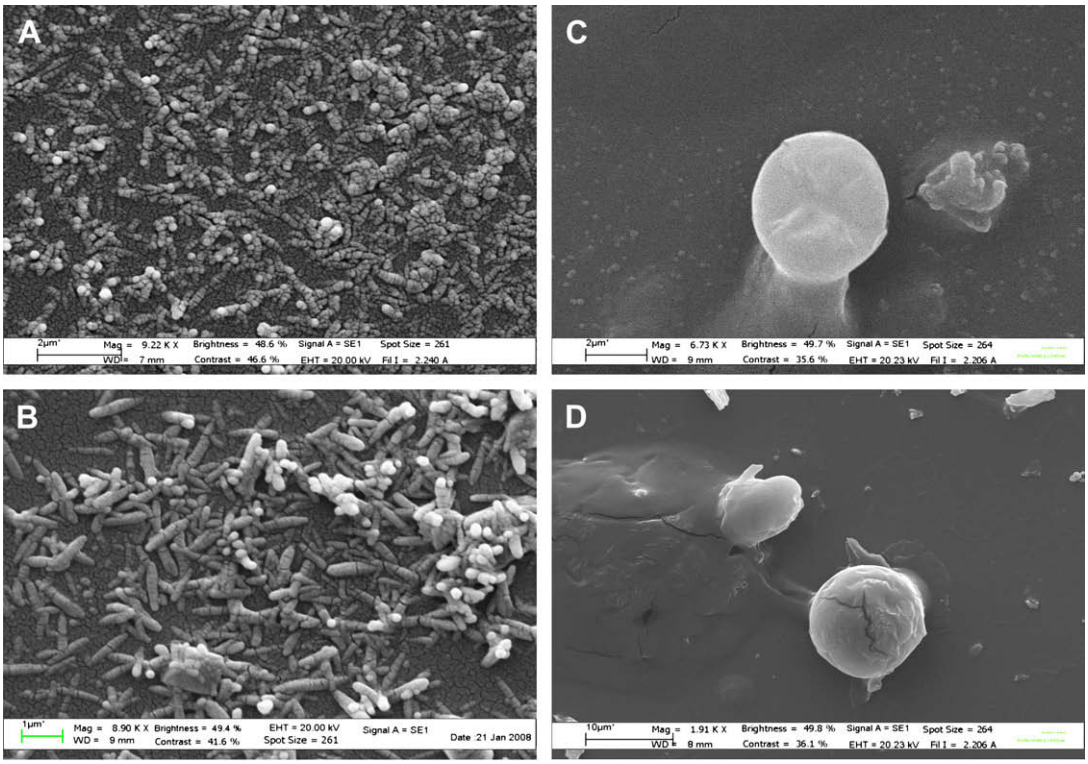

Fig. 2. Effect on $A\beta_{1-40}$ aggregation. SEM images of $A\beta_{1-40}$ (100 μg/100 μL of 30 mM Tris/HCl, pH 7.4) incubated at 20 °C in the absence (A and B) and presence (C and D) of 10 M excess of compound **5**. Aliquots of 5 μL were withdrawn after 30 min (A and C) and 24 h (B and D), frozen, lyophilized and gold coated, by sputtering, prior to SEM analyses.

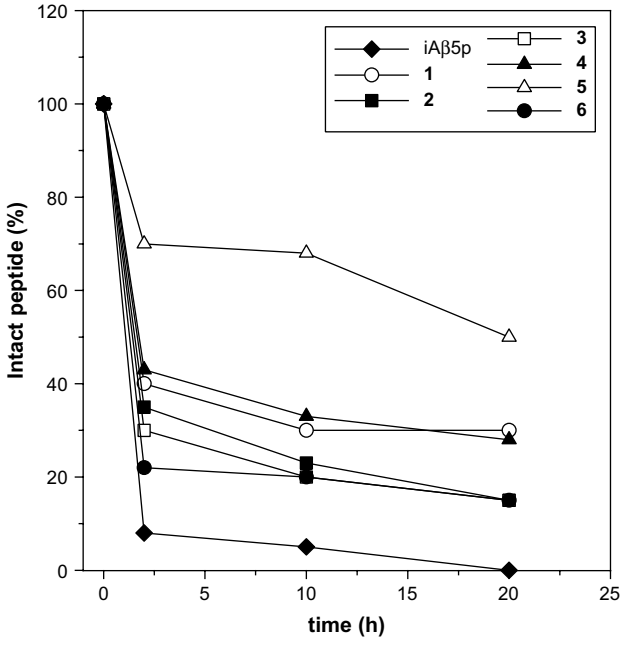

Fig. 3. Patterns of proteolysis of compounds **1**–**6** and iAβ5p by chymotrypsin. Aliquots of iAβ5p and compounds **1**–**6** at a concentration of 0.76 mg/mL were incubated in PBS with 0.1 mg/mL of chymotrypsin at 25 °C. At the desired time, aliquots were withdrawn, added to the same volume of the column elution mixture to stop the reaction and injected on an RP-HPLC column Vydac C_{18}. The area under the peak (UV absorbance at 215 nm) corresponding to the intact peptide was measured and compared with an equivalent sample incubated in PBS.

2.3. Spectroscopic characterization in solution

The peptides have been analyzed by far-UV CD (180–250 nm) (Fig. 4) and by FT-IR in H_2O and in D_2O, respectively (Fig. 5). Far-UV CD spectra of peptides iAβ5p, **2**, **3** and **5** show a weak positive band (n–π*) at around 220 nm and a strong negative band around 200 nm (π–π*), less pronounced for peptide **2**, which can be assigned to polyPro II conformation [32,33]. The iAβ5p and **6** show a weak negative band around 235 nm which can resemble that of β-turn type II [33] and could be attributed to the aromatic contribution to the far-UV CD spectrum [34–36]. Similar redshifted negative (n–π*) bands have been also reported for cyclic peptide and attributed to a composite of class spectrum of II β-turn and the γ-turn [33]. Interestingly, the negative band at 230 nm, present in iAβ5p and in **6**, is absent in spectra of **2**, **3** and **5**. The far-UV CD spectra of **1** and **4**, differently from the other peptides, both show negative ellipticity at around 220 nm; a zero intercept at around 190 nm is detected only for **4**.

The far-UV CD spectra indicate that **2**, **3** and **5** present dichroic activity bands similar to those of the iAβ5p leading structure (Fig. 4). On the other hand, the ellipticity observed for **1** and **4** indicates that the changes in the primary structure have caused significant changes in the secondary structure elements with respect to iAβ5p. Peptides have been also analyzed by FT-IR spectroscopy, in D_2O, in the amide I′, amide II′ and in the spectral region where the side chains of amino acid

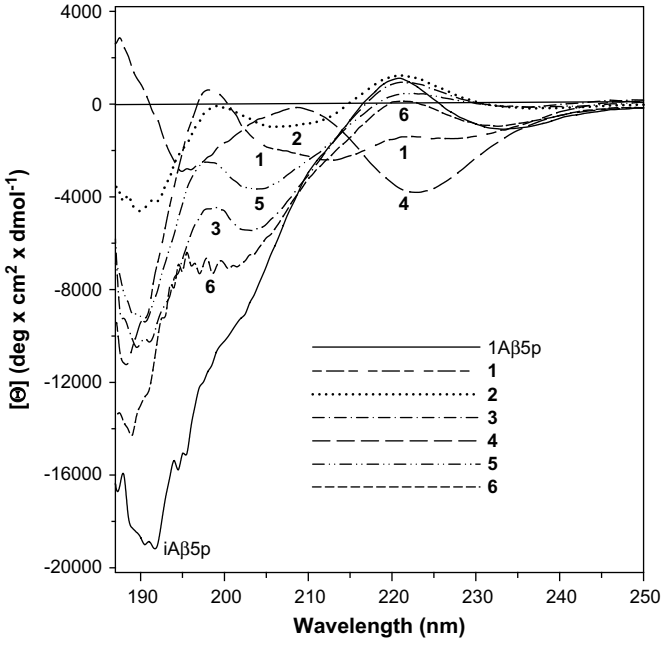

Fig. 4. Far-UV CD spectra of compounds **1**–**6** and iAβ5p. All the spectra were recorded at 20 °C in ultra high quality water.

residues are known to make contributions [37,38] (Fig. 5 and Table 2).

FT-IR absorbance spectrum of iAβ5p shows a maximum centred at 1647 cm^{-1} and a band at 1456 cm^{-1}, corresponding to the amide I′ and amide II′ region, respectively. The amide I′ region presents two significant shoulders at 1671 and 1620 cm^{-1}. In the amide I′ region, the main peak at 1647 cm^{-1} can be assigned to unordered loops [37,39] and the 1671 and 1620 cm^{-1} shoulders to β-turns [37,39] and polyPro II [40], respectively. The region of antisymmetric stretching vibration ν_{as} COO^- mode of the unprotonated carboxyl groups (1595–1550 cm^{-1}) and the region 1430–1390 cm^{-1} corresponding to the symmetric stretching vibration ν_s COO^- mode of the unprotonated carboxyl groups show the typical contributions of the Asp residues [38,39]. The contribution of Phe at 1498 cm^{-1}, Pro at 1470 cm^{-1} and of δ_{as} (CH_3) of Leu at 1440 cm^{-1} is also observed [38,39]. Peptide **6** shows the same bands observed for iAβ5p, except for a decrease in intensity of the shoulder at 1618 cm^{-1}. FT-IR spectra of peptides **1** and **2** show both a significant decrease in the 1672 cm^{-1} and an increase in the 1618 cm^{-1} bands and for peptide **2** the main amide I′ band is broadened and shifted from 1647 to 1640 cm^{-1}. The presence of the 1618 cm^{-1} band in **1** is not paralleled by the typical far-UV CD of polyPro II.

The contributions of amide I′ region in the spectrum of peptide **3** are comparable to those of iAβ5p, except for a decrease in the intensity of the 1618 cm^{-1} band (Fig. 5 and Table 2). Peptides **4** and **5** are characterized by the absence of the contribution of the 1618 cm^{-1} band and by a significant increase in the intensity of the 1672 cm^{-1} band. In the amide II′ region the spectra of all the peptides are comparable and do not show any significant difference. Notably, FT-IR spectra of all the compounds show a decreased content of the unordered loop

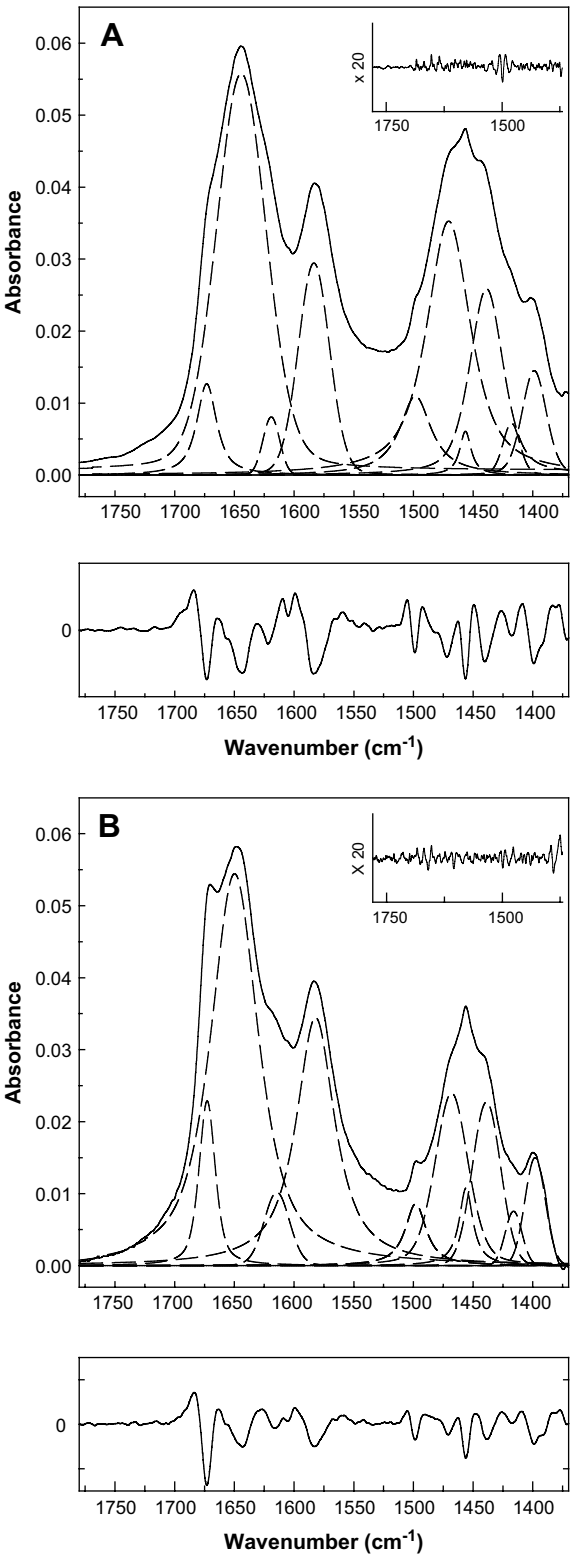

Fig. 5. FT-IR spectra of compounds **1** and **6**. Solution FT-IR spectra were measured at 20 mg/mL compound in ^2H_2O in a CaF_2 cell with a 0.015 mm spacer at 20 °C. A total of 512 interferograms at 2 cm^{-1} resolution were collected for each spectrum. Absorbance spectra of compounds **1** (A) and **6** (B) amides I′ and II′ in ^2H_2O. Deconvolution of the spectra was used to identify the individual components in the amide I′ and amide II′ regions by curve fitting of the raw spectra. The panels show the second derivative of the raw spectra. Insets show the difference between the fitted curve and the original expanded 20 times.

Table 2
Peak position and secondary structure assignment of the amide I′ of compounds **1**–**6** and iAβ5p

Peak position (cm^{-1})	Area (%)							Assignment
	iAβ5p	**1**	**2**	**3**	**4**	**5**	**6**	
1672	4.45	5.08	1.42	10.01	6.14	14.75	5.79	β-Turn
1647	45.9	30.20	25.08	27.10	29.76	26.23	39.90	Unordered loops
1618	4.39	10.02	15.27	11.00	0.04	1.44	3.20	PolyPro II + Pro
1581	18.28	18.61	12.44	14.63	11.14	12.40	22.03	Asp[a]
1498	0.78	0.21	0.18	1.15	4.03	1.13	3.08	Phe
1465	14.78	22.39	23.67	10.10	17.38	8.09	10.62	Pro, Leu[b]
1456	1.61	0.87	0.70	2.47	3.36	11.58	2.63	Amide II′
1440	5.81	6.51	8.70	13.30	14.59	12.50	7.76	Pro, Leu[c]
1416	1.73	2.60	4.05	4.48	7.07	5.74	1.48	Asp[d]
1398	3.09	3.51	8.50	5.95	6.48	6.15	3.65	Asp[d]

[a] ν_{as}(COOH).
[b] $\delta(CH_2)$.
[c] $\delta_{as}(CH_3)$.
[d] ν_s(COOH).

band, as indicated by the decrease in the area at 1647 cm^{-1}, thus suggesting a decreased structural flexibility for all the peptides. The relative content of the β-turn band is decreased in **2** and increased in **3** and **5**. Interestingly, the polyPro II band at 1618 cm^{-1}, which is increased in **1**–**3**, is absent in **4** and decreased in **5**, compounds both including a peptidosulfonamide moiety.

3. Discussion

The formation of insoluble Aβ deposit in the brain is the main pathological trait of Alzheimer's disease. The inhibition of Aβ fibril deposition might slow down or prevent the disease, according to the hypothesis that fibrils mediate neurotoxicity [41]. Hence, the screening for compounds that reduce oligomerization or formation of fibrils could be a discrete target for therapeutics [42].

Replacement of the Pro with the Aze residue in iAβ5p analogue **1** causes an increase of the activity, suggesting that the alteration of the backbone conformation associated with the enhancement of the ring constraint, when combined with reduction of the steric interference exerted by ring atoms [43], improves destabilization of intermolecular β-sheet of Aβ aggregates. By taking into account this finding, the inactivity of compound **2**, containing the (2*R*,3*R*)-PhAze, doesn't appear in contrast with this result and underlines that the non-covalent repulsive interactions exerted by ring atoms and by substituents on the ring, in this crucial point of the molecule, exert an highly unfavorable effect.

A residue of β-amino-carboxylic and of the corresponding β-amino-ethanesulfonic acid, both possessing a pyrrolidine ring, has been incorporated in compounds **3** and **4**, respectively. Although in both these analogues the inherent structural flexibility of the β-residues is limited by the presence of the pyrrolidine ring, this property, combined with the interference exerted by the extra methylene group on the formation of a regular hydrogen bonding network, results to be highly unfavorable for the binding of the inhibitor to Aβ [44].

The consequences on the inhibitory activity of structural modifications performed at the N-terminal protecting group of iAβ5p have been previously examined by Soto's group [15]. Although the results reveal a complex picture, an interesting indication is that iAβ5p analogues possessing sarcosine or *N*-methyl-sarcosine bound at the Leu amino group show the highest activity. On the basis of these findings we synthesized the analogue **5** which maintains the N-terminal tertiary amino group as part of the β-amino-ethanesulfonic fragment bound to the N-terminal Leu residue. In accordance with the previous results [15] the sulfonamide-pseudopeptide **5** shows the highest activity among the here examined pentapeptide derivatives (Fig. 1) and the highest enzymatic stability (Fig. 3). It can be noted here that a significant resistance to the hydrolytic degradation is found also in the case of compound **4** which shares with **5** the presence of the sulfonamide junction in the molecule.

Finally, compound **6** duplicates the iAβ5 sequence and maintains both the C-terminal amide and the *N*-terminal acetyl protecting group. The inhibitory activity of this *N*-acetyl-decapeptide-amide is very high and indicates an improved interaction with the aggregating fibrils. This behaviour can be related to that shown by the peptide dimers (bivalent ligands) and their simultaneous interaction with different points of the receptor [45]. These ligands, when can interact with two proximal recognition sites of the receptor exhibit, due to entropic factors, a considerably greater potency and affinity than the monomeric analogues. In the present case the picture is more complex and strictly related to the interaction mechanism of the dimer with the Aβ molecule. Studies focused on the activity of further new models, designed to contain two monomeric fragments linked or cross-linked by spacers of different length, seem now promising tools to better understand this interesting point.

In summary, the here reported results confirm the value of the peptide fragment individuated by Soto's group as lead compound to generate analogues capable to hinder fibrillogenesis. In particular we find that the enhancement of the

conformational constraint at position 2 of the iAβ5p, induced by the incorporation of the Aze residue (analogue **1**), improves the activity. This effect, however, does not result compatible with substituents on the Aze ring (analogue **2**), thus indicating the key role of the structural modifications at position 2 for tuning the activity of the iAβ5p analogues. Analogously, the high activity of the peptide derivative **5** underlines the usefulness of modifications performed at the N-terminal position and in particular the role that the sulfonamido junction can play in terms of both metabolic stability and alteration of usual H-bond patterns [44]. Finally, the dimeric analogue **6** may represent, as discussed above, the basis for the design of new models to which several of the here reported results can be transferred.

4. Experimental protocols

Melting points were determined with a Büchi B 540 apparatus and are uncorrected. IR spectra were recorded in 1% $CHCl_3$ (unless otherwise specified) solution employing a Perkin–Elmer FT-IR Spectrum 1000 spectrometer. ^{1}H NMR spectra were determined in $CDCl_3$ solution with a Bruker AM 400 spectrometer and chemical shifts were indirectly referred to TMS. The mass spectra were obtained in electrospray (ES) conditions by a ZABSpec oa-TOF (Micromass Ltd., Manchester, UK) instrument. Thin-layer and preparative layer chromatographies were performed on silica gel Merck 60 F_{254} plates. The drying agent was sodium sulfate. Elemental analyses for C, H and N (where necessary a sample was further purified by preparative TLC) were performed in the laboratories of the Servizio Microanalisi del CNR, Area della Ricerca di Roma, Montelibretti, Italy, and were within ±0.4% of the theoretical values.

4.1. Cbz–Pro–ψ[CH_2SO_2]–Cl

Purified by silica gel flash chromatography (CH_2Cl_2). The product was dried (P_2O_5) and stored under argon. Colourless oil (46%). IR ν: 3033, 2957, 2873, 1701 cm^{-1}. ^{1}H NMR δ: 1.92–2.12 (m, 4H, Pro CH_2CH_2), 3.18–3.42 (m, 2H, Pro CH_2N), 3.62–3.76 (m, 2H, CH_2S), 4.61–4.75 (m, 1H, Pro αCH), 5.18 (s, 2H, Cbz CH_2), 7.38 (s, 5H, Ar). Anal. Calcd for $C_{13}H_{16}NO_4ClS$: C, 49.13; H, 5.08; N, 4.41. Found: C, 49.28; H, 4.97; N, 4.33.

4.2. Cbz–Pro–ψ[CH_2SO_2]–Phe–OMe

Purified by silica gel flash chromatography ($CHCl_3$). Colourless oil (48%). IR ν: 3354, 3011, 1743, 1693, 1497, 1436, 1218 cm^{-1}. ^{1}H NMR δ: 1.53–2.18 (m, 4H, Pro CH_2CH_2), 2.45–3.24 (three m, 6H, Phe CH_2, CH_2S and Pro CH_2N), 3.78 (s, 3H, OCH_3), 3.96–4.05 (m, 1H, Pro αCH), 4.30–4.43 (m, 1H, Phe αCH), 4.68–4.82 (m, 1H, SO_2NH), 5.18 (s, 2H, Cbz CH_2), 7.08–7.42 (m, 10H, Ar). Anal. Calcd for $C_{23}H_{28}N_2O_6S$: C, 59.98; H, 6.13; N, 6.08. Found: C, 60.06; H, 6.24; N, 6.17.

4.3. Coupling with carbodiimide

To an ice-cooled mixture containing the required *N*-protected amino acid or peptide (1.0 mmol), the *C*-protected amino acid or peptide salt (1.0 mmol), HOBt (1.2 mmol) and TEA (1.2 mmol) in anhydrous CH_2Cl_2 (6 mL), EDC (1.0 mmol) were added and the reaction mixture was allowed to warm slowly to room temperature overnight. The reaction mixture was then diluted with CH_2Cl_2 (20 mL) and washed with 1 M $KHSO_4$ (2 × 15 mL), saturated aqueous $NaHCO_3$ (2 × 15 mL) and brine (15 mL). The organic phase was dried and evaporated under reduced pressure.

4.3.1. N-Benzyl-(2R,3R)-PhAze-Phe–OMe

Purified on silica gel flash chromatography (hexane/$CHCl_3$ 7:3). Colourless oil (56%). IR ν: 3687, 3356, 3029, 1743, 1668, 1514, 1236 cm^{-1}. ^{1}H NMR δ: 3.00–3.18 (m, 3H, Phe CH_2 and PhCH), 3.48 (d, 1H, $J = 10.0$ Hz, Aze αCH), 3.60–3.82 [m, 7H, Aze CH_2, $PhCH_2$ and OCH_3 (s at 3.76)], 4.90 (m, 1H, Phe αCH), 7.08–7.40 (m, 15H, Ar), 7.81 (d, 1H, $J = 6.0$ Hz, NH). Anal. Calcd for $C_{27}H_{28}N_2O_3$: C, 75.68; H, 6.59; N, 6.54. Found: C, 75.73; H, 6.57; N, 6.49.

4.3.2. Cbz–β-HPro-Phe–OMe

Purified on silica gel flash chromatography (EtOAc/Et_2O). Colourless oil (65%). IR ν: 3686, 3420, 3010, 1741, 1685, 1514, 1418, 1226 cm^{-1}. ^{1}H NMR δ: 1.82–2.23 (m, 4H, Pro CH_2–CH_2), 2.88–3.22 (two m, 4H, Phe CH_2 and Pro CH_2N), 3.20 (br s, 2H, CH_2CO), 3.64 (s, 3H, OCH_3), 4.22–4.38 (m, 1H, Pro αCH), 4.88–4.95 (m, 1H, Phe αCH), 5.16 (s, 2H, Cbz CH_2), 6.48 (br s, 1H, NH), 7.00–7.41 (m, 10H, Ar). Anal. Calcd for $C_{24}H_{28}N_2O_5$: C, 67.91; H, 6.65; N, 6.60. Found: C, 67.85; H, 6.72; N, 6.53.

4.3.3. Cbz–Phe-Asp(O^tBu)–NH_2

White solid (80%). IR ν: 3685, 3402, 3034, 1724, 1498, 1156 cm^{-1}. ^{1}H NMR (DMSO-d_6) δ: 1.40 [s, 9H, $(CH_3)_3C$], 2.40–2.82 [m, 3H, Phe CH_2 (1H) and Asp CH_2], 2.87–3.14 [m, 1H, Phe CH_2 (1H)], 4.22 (m, 1H, Phe αCH), 4.50 (m, 1H, Asp αCH), 4.95 (s, 2H, Cbz CH_2), 7.02–7.38 (m, 10H, Ar), 7.55 (d, 1H, $J = 7.5$ Hz, Phe–NH), 8.22 (d, 1H, $J = 7.5$ Hz, Asp–NH). Anal. Calcd for $C_{25}H_{31}N_3O_6$: C, 63.95; H, 6.65; N, 8.95. Found: C, 63.77; H, 6.59; N, 8.82.

4.3.4. N-Benzyl-(2R,3R)-PhAze-Phe-Phe-Asp(O^tBu)–NH_2

Crystallized from EtOAc. White solid (86%). IR ν: 3658, 3401, 3034, 1674, 1497, 1200 cm^{-1}. ^{1}H NMR δ: 1.39 [s, 9H, $(CH_3)_3C$], 2.58–3.15 (m, 5H, 2 × Phe CH_2 and PhCH), 3.85–4.03 (m, 7H, Aze CH_2, $PhCH_2$, Asp CH_2 and Aze αCH), 4.10–4.64 (three m, 3H, 2 × Phe αCH and Asp αCH), 6.98–7.51 (m, 20H, Ar). Anal. Calcd for $C_{43}H_{49}N_5O_6$: C, 70.57; H, 6.77; N, 9.57. Found: C, 70.64; H, 6.69; N, 9.71.

4.3.5. Cbz–Aze-Phe-Phe-Asp(O^tBu)–NH_2

Triturated with hexane. White solid (86%). IR ν: 3676, 3400, 3022, 1685, 1517, 1234, 1156 cm^{-1}. ^{1}H NMR δ: 1.41

[s, 9H, $(CH_3)_3C$], 2.19–2.43 (m, 2H, CH_2CH_2CH), 2.56–3.21 (m, 6H, 2 × Phe CH_2 and Asp CH_2), 3.65–3.80 and 3.84–4.01 (two m, 2H, CH_2CH_2CH), 4.45–4.60 and 4.71–4.82 (two m, 4H, 4 × αCH), 5.10 (s, 2H, Cbz CH_2), 5.21 (br s, 1H, NH), 6.39 (br s, 1H, NH), 6.70 (d, 1H, $J = 8.0$ Hz, NH), 7.20–7.41 (m, 15H, Ar). Anal. Calcd for $C_{38}H_{45}N_5O_8$: C, 65.22; H, 6.48; N, 10.01. Found: C, 65.34; H, 6.57; N, 9.88.

4.3.6. Cbz–β-HPro-Phe-Phe-Asp(O^tBu)–NH_2

Crystallized from EtOAc/hexane. White solid (77%). IR ν: 3692, 3402, 3036, 1681, 1498, 1236, 1157 cm^{-1}. ^1H NMR δ: 1.40 [s, 9H, $(CH_3)_3C$], 1.64–2.18 (m, 4H, Pro CH_2CH_2), 2.83–3.20 (m, 8H, 2 × Phe CH_2, Pro CH_2N and Asp CH_2), 3.22–3.51 (m, 2H, Pro CH_2CO), 4.15–4.98 (four m, 4H, 4 × αCH), 5.16 (s, 2H, Cbz CH_2), 5.40, 6.37 and 6.66 (three br s, 3H, 3 × NH), 7.05–7.42 (m, 15H, Ar). Anal. Calcd for $C_{40}H_{49}N_5O_8$: C, 66.01; H, 6.79; N, 9.62. Found: C, 66.18; H, 6.65; N, 9.48.

4.3.7. Cbz–Pro–ψ[CH_2SO_2]–Phe-Phe-Asp(O^tBu)–NH_2

Pale yellow oil (55%). IR ν: 3689, 3400, 3014, 1689, 1498, 1199 cm^{-1}. ^1H NMR δ: 1.43 [s, 9H, $(CH_3)_3C$], 1.72–2.08 (m, 4H, Pro CH_2CH_2), 2.41–3.25 (m, 10H, 2 × Phe CH_2, Pro CH_2N, Asp CH_2 and CH_2SO_2), 4.43–4.82 (m, 4H, 4 × αCH), 5.15 (s, 2H, Cbz CH_2), 5.62 and 5.73 (two br s, 2H, 2 × NH), 6.31 (d, 1H, $J = 8.2$ Hz, NH), 7.09–7.38 (m, 15H, Ar). Anal. Calcd for $C_{39}H_{49}N_5O_9S$: C, 61.32; H, 6.47; N, 9.17. Found: C, 61.17; H, 6.62; N, 9.05.

4.3.8. Cbz–Tau-Leu-Pro-Phe–OMe

White solid (54%). IR ν: 3675, 3409, 3032, 1668, 1512, 1356, 1212, 1150 cm^{-1}. ^1H NMR δ: 1.02–1.30 (m, 6H, Leu CH_3), 1.42–1.61 (m, 3H, Leu CH_2CH), 1.70–2.19 (m, 4H, Pro CH_2CH_2), 2.20–2.37 (m, 2H, Tau αCH$_2$), 2.87–3.08 (m, 2H, Pro CH_2N), 3.10–3.41 (m, 2H, Tau βCH$_2$), 3.60–3.82 (m, 2H, Phe CH_2), 3.90 (s, 3H, OCH_3), 4.12–4.82 (three m, 3H, 3 × αCH), 5.36 (s, 2H, Cbz CH_2), 5.80, 5.98 (two m, 2H, 2 × NH), 7.18 (d, 1H, $J = 6.0$ Hz, NH), 7.30–7.65 (m, 10H, Ar). Anal. Calcd for $C_{31}H_{42}N_4O_8S$: C, 59.03; H, 6.71; N, 8.88. Found: C, 59.19; H, 6.57; N, 8.71.

4.3.9. Cbz–Tau-Leu-Pro-Phe-Phe-Asp(O^tBu)–NH_2

Purified on silica gel flash chromatography ($CHCl_3$/MeOH 98:2). White solid (40%). IR ν: 3675, 3398, 3015, 1670, 1521, 1398, 1212, 1148 cm^{-1}. ^1H NMR δ: 1.12–1.22 (m, 6H, Leu CH_3), 1.52–1.65 [m, 12H, Leu CH_2CH and $C(CH_3)_3$ (s at 1.62)], 1.98–2.38 (m, 6H, Pro CH_2CH_2 and Asp CH_2), 3.00 (d, 2H, $J = 7.2$, Tau αCH$_2$), 3.14–3.58 (m, 6H, Pro CH_2N and 2 × Phe CH_2), 3.60–3.78 (m, 1H, αCH), 3.80–3.98 (m, 2H, Tau βCH$_2$), 4.28–5.19 (four m, 4H, 4 × αCH), 5.37 (s, 2H, Cbz CH_2), 5.38 (d, 1H, $J = 6.1$ Hz, NH), 5.93 (m, 1H, NH), 5.83–6.04 [m, 2H, $CONH_2$ (1H) and NH], 6.28 (d, 1H, $J = 6.3$ Hz, NH), 6.70–6.82 [m, 1H, $CONH_2$ (1H)], 7.20–7.62 (m, 16H, Ar and NH). Anal. Calcd for $C_{47}H_{63}N_7O_{11}S$: C, 60.43; H, 6.80; N, 10.50. Found: C, 60.28; H, 6.75; N, 10.23.

4.3.10. Ac–Leu-Aze-Phe-Phe-Asp(O^tBu)–NH_2

Triturated with hexane. White solid (62%). IR ν: 3326, 3009, 1673, 1513, 1369, 1235, 1156 cm^{-1}. ^1H NMR δ: 0.89–0.98 (m, 6H, Leu CH_3), 1.19–1.75 [m, 12H, Leu CH_2CH and $(CH_3)_3C$ (s at 1.40)], 1.98 (s, 3H, CH_3CO), 2.22–2.43 (m, 2H, CH_2CH_2CH), 2.52–3.15 (m, 6H, 2 × Phe CH_2 and Asp CH_2), 3.80–3.96 (m, 2H, CH_2CH_2CH Aze CH_2), 4.21–4.80 (m, 5H, 5 × αCH), 5.40 [s, 1H, $CONH_2$ (1H)], 6.08 (d, 1H, $J = 8.4$ Hz, Leu NH), 6.42 [s, 1H, $CONH_2$ (1H)], 6.70 (d, 1H, $J = 8.0$ Hz, Phe NH), 6.98 (d, 1H, $J = 7.8$ Hz, Phe NH), 7.04–7.31 (m, 10H, Ar), 7.82 (d, 1H, $J = 7.5$ Hz, Asp NH). Anal. Calcd for $C_{38}H_{52}N_6O_8$: C, 63.32; H, 7.27; N, 11.66. Found: C, 63.30; H, 7.22; N, 11.75.

4.3.11. Ac–Leu-(2R,3R)-PhAze-Phe-Phe-Asp(O^tBu)–NH_2

Triturated with hexane. White solid (58%). IR ν: 3331, 3017, 1673, 1498, 1236, 1156 cm^{-1}. ^1H NMR δ: 0.92–1.03 (m, 6H, Leu CH_3), 1.22–1.73 [m, 12H, Leu CH_2CH and $(CH_3)_3C$ (s at 1.40)], 2.00 (s, 3H, CH_3CO), 2.63–3.26 (m, 7H, 2 × Phe CH_2, PhCH and Asp CH_2), 3.63–3.76 (m, 2H, Aze CH_2), 4.18–4.26 and 4.41–4.80 (two m, 5H, 5 × αCH), 5.50 [br s, 1H, $CONH_2$ (1H)], 6.18 (br s, 1H, Leu NH), 6.37 [s, 1H, $CONH_2$ (1H)], 6.64 (br s, 1H, Phe NH), 7.04–7.56 (m, 17H, Ar, Phe NH and Asp NH). Anal. Calcd for $C_{44}H_{56}N_6O_8$: C, 66.31; H, 7.08; N, 10.55. Found: C, 66.17; H, 7.23; N, 10.48.

4.3.12. Ac–Leu-β-HPro-Phe-Phe-Asp(O^tBu)–NH_2

Triturated with hexane. White solid (67%). IR ν: 3690, 3411, 2930, 1709, 1498, 1369, 1222, 1156 cm^{-1}. ^1H NMR δ: 0.86–1.08 (m, 6H, Leu CH_3), 1.17–1.78 [m, 12H, Leu CH_2CH and $(CH_3)_3C$ (s at 1.42)], 1.80–2.12 [m, 7H, Pro CH_2CH_2 and CH_3CO (s at 1.97)], 2.66–2.88 (m, 2H, Asp CH_2), 2.89–3.25 (m, 4H, 2 × Phe CH_2), 3.28–3.46 (m, 2H, Pro CH_2CO), 3.60–3.98 (m, 2H, Pro CH_2N), 4.20–4.95 (five m, 5H, 5 × αCH), 5.43 [s, 1H, $CONH_2$ (1H)], 5.80 (br s, 1H, Leu NH), 6.63 [s, 1H, $CONH_2$ (1H)], 6.78 (br s, 1H, Phe NH), 7.00–7.43 (m, 11H, Ar and Phe NH), 7.65 (br s, 1H, Asp NH). Anal. Calcd for $C_{40}H_{56}N_6O_8$: C, 64.15; H, 7.54; N, 11.22. Found: C, 64.10; H, 7.63; N, 11.03.

4.3.13. Ac–Leu-Pro–ψ[CH_2SO_2]–Phe-Phe-Asp(O^tBu)–NH_2

Triturated with hexane. White solid (67%). IR ν: 3689, 3401, 3027, 1673, 1509, 1396, 1202, 1153 cm^{-1}. ^1H NMR δ: 0.87–1.05 (m, 6H, Leu CH_3), 1.29–1.74 [m, 12H, Leu CH_2CH and $(CH_3)_3C$ (s at 1.46)], 1.86–2.18 [m, 7H, Pro CH_2CH_2 and CH_3CO (s at 2.02)], 2.88–3.24 (m, 8H, 2 × Phe CH_2, Asp CH_2 and CH_2SO_2), 3.48–3.67 (m, 2H, Pro CH_2N), 4.10–4.26, 4.62–4.68, 4.70–4.79 and 4.96–5.04 (four m, 5H, 5 × αCH), 5.32 [s, 1H, $CONH_2$ (1H)], 5.50 (br s, 1H, Leu NH), 6.10 (d, 1H, $J = 6.9$ Hz, Phe NH), 6.32 [br s, 1H, $CONH_2$ (1H)], 7.03 (d, 1H, $J = 6.5$ Hz, Phe NH), 7.10–7.32 (m, 10H, Ar), 7.42 (d, 1H, $J = 6.8$ Hz, Asp NH). Anal. Calcd for $C_{39}H_{56}N_6O_9S$: C, 59.67; H, 7.19; N, 10.71. Found: C, 59.52; H, 7.24; N, 10.63.

4.4. N,N-Dimethyl-Tau-Leu-Pro-Phe-Phe-Asp(O^tBu)–NH_2

Triturated with hexane. White solid (quantitative). IR ν: 3667, 3421, 3023, 1667, 1500, 1391, 1220, 1143 cm^{-1}. ^1H NMR (DMSO-d_6) δ: 0.73–0.95 (m, 6H, Leu CH_3), 1.58–1.75 [m, 12H, Leu CH_2CH and $C(CH_3)_3$ (s at 1.60)], 2.38–2.52 [m, 12H, Pro CH_2CH_2, Asp CH_2 and $(CH_3)_2N$ (s at 2.43)], 2.54 (d, 2H, $J = 6.80$ Hz, Tau αCH_2), 2.62–3.50 (m, 8H, Pro CH_2N, $2 \times$ Phe–CH_2 and Tau βCH_2), 3.98–4.54 (five m, 5H, $5 \times \alpha CH$), 6.81–7.27 [m, 11H, Ar and $CONH_2$ (1H)], 7.83, 8.04, 8.18 (three m, 3H, $3 \times$ NH), 8.32 [s, 1H, $CONH_2$ (1H)], 8.40 (m, 1H, NH). Anal. Calcd for $C_{41}H_{61}N_7O_9S$: C, 59.47; H, 7.43; N, 11.84. Found: C, 59.62; H, 7.38; N, 11.75.

4.5. Amyloid detection in suspension

$A\beta_{1-40}$ (lots MZ09356, MZ13377 and MZ13736) was purchased from NeoMPS (Strasbourg, France). The pretreatment of $A\beta_{1-40}$ using the dissolution protocol in NaOH [22] was used because this pretreatment was shown to facilitate amyloid fibril formation. Typically, a 1 mg batch of $A\beta_{1-40}$ (around 2×10^{-4} mol with six acid equivalents) was added with no more than 400 μL of 0.1 M NaOH (4×10^{-5} equiv OH^-), sonicated in a water bath at room temperature and then added with 1100 μL of MilliQ water to reach a final concentration of 0.67 mg/mL; the pH (Merck neutralyt) was around 7.5 and the peptide was completely solubilized. The amount of NaOH could be less than 4×10^{-5} equiv depending on the batch. This sample was divided into several fractions, each containing about 100 μg of $A\beta_{1-40}$, frozen and lyophilised. Each compound (**1**–**6** and iAβ5p) was dissolved with the minimum amount of NaOH to titrate the solution to around pH 8.0 (Merck, neutralyt), buffered with 0.1 M Tris/HCl at pH 7.4 and then stored frozen at 3–4 mM. The incubation mixture for amyloid fibril formation was prepared by dissolving each lyophilised $A\beta_{1-40}$ fraction (about 100 μg) with 100 μL of 30 mM Tris/HCl buffer at pH 7.4 at 20 °C with and without 10 M excess of compound (**1**–**6** and iAβ5p) to be tested as an inhibitor. The amyloid fibril formation was tested according to LeVine [28] with minor modifications. To detect and quantify the formation of amyloid fibrils, a 5 and 10 μL aliquots of the incubation mixture, in the presence and absence of the inhibitor, were withdrawn at increasing incubation times (0.5, 1.5, 6.0, 8.0, 15 and 24 h), and added separately to two cuvettes containing 1 mM ThT each in 50 mM Tris/HCl buffer, pH 8.0 at 20 °C. All experiments were repeated three times and each sample was analyzed in triplicates. Fluorescence emission spectra (460–550 nm) were measured at 20 °C in a Perkin–Elmer LS50B fluorimeter with excitation set at 450 nm immediately after addition of the incubation mixture. The plots of the relative fluorescence at 485 nm as a function of the incubation times (data not shown) indicate that in all the experiments the relative fluorescence observed remained constant after 15 h incubation.

4.6. Scanning electron microscopy studies

Morphologies of $A\beta_{1-40}$ were investigated using a scanning electron microscopy (SEM) LEO 1450VP with tungsten filament as electron emitter with 20 keV acceleration potential and a resolution of 4 nm. For the SEM study, samples of $A\beta_{1-40}$ incubated in the absence and presence of inhibitors in the same conditions as those described for amyloid detection in suspension (see Section 4.5) were withdrawn at different times, frozen, lyophilised and gold coated.

4.7. Proteolytic assays

Aliquots of iAβ5p and analogues at a concentration of 0.76 mg/mL in phosphate buffer saline (PBS) were incubated over increasing time with 0.1 mg/mL of chymotrypsin (Fluka) at 25 °C. At the desired time, aliquots were withdrawn and added to the same volume of the column elution mixture to stop the reaction. This sample was immediately injected on an RP-HPLC column (Vydac C_{18}, 0.46×25 cm) and eluted with an isocratic system (acetonitrile/water 80:20). The area of the peak (UV absorbance at 215 nm) corresponding to the intact peptide was measured and compared with an equivalent sample incubated in PBS.

4.8. Spectroscopy

Compounds **1**–**6** and iAβ5p were dissolved as described in Section 4.5, lyophilized and stored at −20 °C before spectral measurements. Far-UV CD (180–250 nm) measurements were performed at 20 °C in 0.01–0.1 cm path length quartz cuvettes on each lyophilized compound dissolved in ultra high quality water. CD spectra were recorded on a Jasco J-720 spectropolarimeter. The results are expressed as the mean residue ellipticity [Θ] assuming a mean residue weight of 110 per amino acid residue. FT-IR spectra in the amide I′ and amide II′ regions were recorded on a Nicolet Magna 760 spectrometer (Thermo Nicolet, Madison, WI, USA) equipped with a liquid nitrogen-cooled mercury–cadmium telluride solid-state detector. FT-IR transmission spectra of about 20 mg/mL peptides in ^2H_2O were measured in a CaF_2 cell with a 0.015 mm spacer (Spectra Tech, Madison, WI, USA) at 20 °C. For exchange of amide protons with deuterons, each lyophilized compound (**1**–**6** and iAβ5p) was dissolved in ^2H_2O, freeze-dried and dissolved three times in ^2H_2O at 20 °C before measurements. A total of 512 interferograms at 2 cm^{-1} resolution were collected for each spectrum, with Mertz apodization and two levels of zero filling. The sample chamber of the spectrometer was continuously purged with dry air to avoid water vapor interference on the bands of interest. The background spectra were collected immediately before the sample measurements and under the same conditions with the cell filled with everything but peptide sample. Water vapor spectra were collected by reduction of the dry-air purge of the clean cell. The analysis of raw spectra was performed with GRAMS (Galactic Industries Corp., Salem, NH). The water vapor contribution was subtracted from each of the sample

spectra. The essentially featureless region between 1700 and 1800 cm^{-1} (where no peptide bands are present) indicated that water vapor components are not responsible for the observed bands in the amide I′ region. The individual components in the amide region were identified by second derivative and Fourier self-deconvolution of the raw spectrum using GRAMS. Curve fitting of the raw spectrum with a mixed Gaussian–Lorentzian function was then performed to determine the peak positions and parameters of each individual component. The assignments of the component bands to secondary structure elements were based on the literature [37–39], and the area under each peak was used to calculate the percentage of secondary structure components (Table 2).

References

[1] L.C. Serpell, Biochim. Biophys. Acta 1502 (2000) 16–30.
[2] C. Adessi, C. Soto, Drug Dev. Res. 56 (2002) 184–193.
[3] C. Soto, M.E. Castano, B. Frangione, N.C. Inestrosa, J. Biol. Chem. 270 (1995) 3063–3067.
[4] J. Ghanta, C.L. Shen, L.L. Kiessling, R.M. Murphy, J. Biol. Chem. 271 (1996) 29525–29528.
[5] C. Soto, M.S. Kindi, M. Baumann, B. Frangione, Biochem. Biophys. Res. Commun. 226 (1996) 672–680.
[6] D. Gordon, S.C. Meredith, Biochemistry 42 (2003) 475–485.
[7] R.J. Chalifour, R.W. McLaughlin, L. Lavoie, C. Morissette, N. Tremblay, M. Boulé, P. Sarazin, D. Stéa, D. Lacombe, P. Tremblay, F. Gervais, J. Biol. Chem. 278 (2003) 34874–34881.
[8] F. Yang, G.P. Lim, A.N. Begum, O.J. Ubeda, M.R. Simmons, S.S. Ambegaokar, P.P. Chen, R. Kayed, C.G. Glabe, S.A. Frautschy, G.M. Cole, J. Biol. Chem. 280 (2005) 5892–5901.
[9] T. Cohen, A. Frydman-Marom, M. Rechter, E. Gazit, Biochemistry 45 (2006) 4727–4735.
[10] N. Kokkoni, K. Stott, H. Amijee, J.M. Mason, A.J. Doig, Biochemistry 45 (2006) 9906–9918.
[11] T. Sato, P. Kienlen-Campard, M. Ahmed, W. Liu, H. Li, J.I. Elliott, S. Aimoto, S.N. Constantinescu, J.-N. Octave, S.O. Smith, Biochemistry 45 (2006) 5503–5516.
[12] M. Torok, M. Abid, S.C. Mhadgut, B. Torok, Biochemistry 45 (2006) 5377–5383.
[13] C. Soto, Mol. Med. Today 5 (1999) 343–350.
[14] C. Hilbich, B. Kister-Woike, J. Reed, C.L. Masters, K. Beyreuther, J. Mol. Biol. 228 (1992) 460–473.
[15] C. Adessi, M.J. Frossard, C. Boissard, S. Fraga, S. Bieler, T. Ruckle, F. Vilbois, S.M. Robinson, M. Mutters, W.A. Banks, C. Soto, J. Biol. Chem. 278 (2003) 13905–13911.
[16] B. Permanne, C. Adessi, G.P. Saborio, S. Fraga, M.J. Frossard, J. Van Dorpe, I. Dewachter, W.A. Banks, F. Van Leuven, C. Soto, FASEB J. 16 (2002) 860–862.
[17] C. Soto, E.M. Sigurdsson, L. Morelli, R.A. Kumar, E.M. Castano, B. Frangione, Nat. Med. 4 (1998) 822–826.
[18] S.J. Wood, R. Wetzel, J.D. Martin, M.R. Hurle, Biochemistry 34 (1995) 724–730.
[19] F. Couty, G. Evano, M. Vargas-Sanchez, G. Bouzas, J. Org. Chem. 70 (2005) 9028–9031.
[20] S. Abele, K. Vogali, D. Seebach, Helv. Chim. Acta 82 (1999) 1539–1558.
[21] R.M.J. Liskamp, J.A.W. Kruijtzer, Mol. Divers. 8 (2004) 79–87.
[22] C. Giordano, G. Lucente, A. Mollica, M. Nalli, G. Pagani Zecchini, M. Paglialunga Paradisi, E. Gavuzzo, F. Mazza, S. Spisani, J. Pept. Sci. 10 (2004) 510–523.
[23] S.F. Nelsen, G.R. Weisman, Tetrahedron Lett. 26 (1973) 2321–2324.
[24] F. Couty, G. Evano, N. Ribasso, Tetrahedron: Asymmetry 14 (2003) 2407–2412.
[25] D. Braghiroli, R. Avallone, M. Di Bella, Tetrahedron: Asymmetry 8 (1997) 2209–2213.
[26] A.J. Brouwer, C.F. Monnee, R.M.J. Liskamp, Synthesis (2000) 1579–1584.
[27] E. Atherton, R.C. Sheppard, Solid Phase Synthesis – A Practical Approach, IRL Press, Oxford, 1989.
[28] H. LeVine, Protein Sci. 2 (1993) 404–410.
[29] Y. Fezoui, D.M. Hartley, J.D. Harper, R. Khurana, D.M. Walsh, M.M. Condron, D.J. Selkoe, P.T. Lansbury Jr., A.L. Fink, D.B. Teplow, Amyloid 7 (2000) 166–178.
[30] C. Goldsbury, P. Frey, V. Olivieri, U. Aebi, S.A. Müller, J. Mol. Biol. 352 (2005) 282–298.
[31] R.A. Moore, S.F. Hayes, E.R. Fischer, S.A. Priola, Biochemistry 46 (2007) 7079–7087.
[32] K. Ma, L. Kann, K. Wang, Biochemistry 40 (2001) 3427–3438.
[33] A. Perczel, M. Hollosi, in: G.D. Fasman (Ed.), Circular Dichroism and the Conformational Analysis of Biomolecules, Plenum Press, New York, 1996, pp. 285–380.
[34] R.W. Woody, A.K. Dunker, in: G.D. Fasman (Ed.), Circular Dichroism and the Conformational Analysis of Biomolecules, Plenum Press, New York, 1996, pp. 109–157.
[35] B. Bochicchio, A. Pepe, A.M. Tamburro, Chirality 17 (2005) 364–372.
[36] S. Vuilleumier, J. Sancho, R. Loewenthal, A.R. Fersht, Biochemistry 32 (1993) 10303–10313.
[37] M. Jackson, H.H. Mantsch, Crit. Rev. Biochem. Mol. Biol. 30 (1995) 95–120.
[38] A. Barth, Prog. Biophys. Mol. Biol. 74 (2000) 141–173.
[39] A. Barth, C.Q. Zscherp, Rev. Biophys. 35 (2002) 369–430.
[40] Y. Pilpel, O. Bogin, V. Brumfeld, Z. Reich, Biochemistry 42 (2003) 3519–3526.
[41] C. Rivière, T. Richard, L. Quentin, S. Krisa, J.M. Mérillon, J.P. Monti, Bioorg. Med. Chem. 15 (2007) 1160–1167.
[42] D.J. Selkoe, Nature 399 (1999) A23–A31.
[43] A. Zagari, G. Nemethy, H.A. Scheraga, Biopolymers 30 (1990) 951–959.
[44] R.C. Elgersma, T. Meijneke, R. de Jong, A.J. Brouwer, G. Postuma, T.S. Dirk, D.T. Rijkers, R.M. Liskamp, J. Org. Biomol. Chem. 4 (2006) 3587–3597.
[45] D. Cussac, M. Vidal, C. Leprince, W. Liu, F. Cornille, G. Tiraboschi, B.P. Roques, C. Garbay, FASEB J. 13 (1999) 31–38.